2-Rev.

Pulsed Irradiation of Optimized, MBE Grown, AlGaAs/GaAs Radiation Hardened Photodiodes*

By J.J.Wiczer, T.A. Fischer, L.R. Dawson, G.C. Osbourn, T.E. Zipperian and C.E. Barnes

Sandia National Laboratories
Albuquerque, N.M. 87185

CONF-840712--2-Rev.

DE84 014984

Abstract

An AlGaAs/GaAs double heterojunction, mesa isolated, photodiode grown by molecular beam epitaxy was irradiated with 18 MeV electrons, 1 - 10 MeV x-rays, and neutrons from a pulsed reactor. Test results indicate that the AlGaAs/GaAs photodiodes generate approximately 10 - 20 times less photocurrent during exposure to a pulse of ionizing-radiation than radiation hardened silicon PIN photodiodes. Studies of neutron induced permanent damage in the AlGaAs/GaAs photodiode show only small changes in optical responsivity and a factor of 8 increase in leakage currents after exposure to 3.6 x 10^{15} neutrons/cm^2 and 900 krad gamma. The silicon PIN photodiode was exposed to only 28% of the fluence used on the AlGaAs photodiodes and we observed a 40% decrease in optical responsivity and a factor of 7000 increase in leakage current.

Introduction

Optoelectronic components have become important elements in modern electronic systems due to the many intrinsic advantages of optical signal transfer especially the large available bandwidths, high immunity to electromagnetic interference, and light weight. Many military and space applications require the use of optoelectronic components that continue to operate during and after exposure to a wide variety of ionizing-radiation environments. In these environments, the photodetector element is often the component most sensitive to ionizing-radiation in the optoelectronic subsystem.

An AlGaAs/GaAs double heterojunction photodiode structure designed to be less susceptible to the disrupting effects of ionizing-radiation pulses was fabricated and tested. In the past, we have shown that AlGaAs/GaAs direct bandgap semiconductor devices are intrinsically less susceptible to the effects of ionizing-radiation when compared to indirect bandgap semiconductor materials such as silicon. This effect

* This work was performed at Sandia National Laboratories supported by the U.S. Department of Energy under contract #DE-AC-04-76DP00789

is the result of the large optical absorption coefficients (and thus small active region thickness) associated with direct bandgap materials. Previously, we have reported on the effects of gamma and x-ray irradiation of photodiode structures fabricated with a liquid phase epitaxy process[1,2,3].

In this paper, we report on studies of the effects of neutron irradiation and high energy electron irradiation of specially designed "rad-hard" photodiodes. An AlGaAs/GaAs double heterojunction photodiode grown by molecular beam epitaxy (MBE) will be discussed in detail and results of neutron, electron, and x-ray irradiations will be presented. A thin active layer, epitaxially grown, silicon photodiode was also studied; some preliminary results from these neutron irradiation studies will be presented here.

AlGaAs/GaAs Photodiode Structure

Optimized, mesa isolated, AlGaAs/GaAs double heterojunction photodiodes were grown by the molecular beam epitaxy process. A cross-sectional diagram of the structure is shown in Figure 1. These photodiodes were grown on n-type GaAs, Bridgman substrates approximately 350 microns thick, doped with silicon to 6 x $10^{17}/cm^3$, and characterized with an etch pit density of $3000/cm^2$. A thin (approximately 0.1-0.5 microns) GaAs buffer layer is grown on top of the GaAs substrate to isolate substrate crystallographic imperfections from the active region of the device. Next a 0.2 micron thick n-type $Al_{.3}Ga_{.7}As$ layer with $10^{18}/cm^3$ silicon doping is grown. This layer forms a heterojunction with the GaAs substrate to isolate carriers generated by ionizing-radiation in the substrate region away from the electrical junction depletion region. The third layer above the substrate is the 0.7 micron thick, n-type, silicon doped ($10^{16}/cm^3$) GaAs, optically active region. In this layer, the optical photons of interest are absorbed and generate electron-hole pairs. These optically generated carriers are collected under the influence of the internal electric fields and contribute to the signal current. The fourth layer on top of the substrate is a 0.5 micron thick layer of $Al_{.3}Ga_{.7}As$, p-type, Be doped ($10^{18}/cm^3$) window material. This window layer transmits the optical photons of interest to the GaAs active region. With this configuration the effects of surface recombination are spatially mitigated. In order to prevent debiasing effects, care must be taken to assure that the lateral resistivity of this layer is sufficient for the anticipated signal current. The fifth (top) layer above the GaAs substrate is a 0.4 micron thick, p+, GaAs contacting layer doped with Be to $10^{18}/cm^3$. This layer is removed with photolithography and selective etchants from all regions not covered by contact metallization. The contacting layer provides for the formation of ohmic contacts to the p-side of the photodiode with greater reliability.

Next, a circular region is photolithographically defined and then a sulfuric acid/ hydrogen peroxide/ water etchant is used to create a 6 micron tall, circular mesa active region. The mesa structure is used to eliminate the effects of saw damage at the edges of the device die and reduce edge breakdown effects. A 0.7 micron thick germanium/ gold/ nickel/ gold metallization is deposited on the substrate (bottom) side of the wafer and a 0.7 micron thick gold/ beryllium alloy is deposited on the top surface. Lift-off photolithography is used to define the top contacting ring. After this contacting ring is deposited on the photodiode, the top GaAs layer is selectively removed from all regions not covered by metal with an ammonium hydroxide/ hydrogen peroxide etchant. The devices were mounted on TO-18, headers and covered with glass window, kovar caps. No anti-reflection coatings were used in these research devices. Anti-reflection coating reduce the amount of light reflected at the surface of the detector due to index of refraction mismatches at the air-semiconductor interface. This technology is well known but was not available during the processing of these devices.

Silicon PIN Photodiode Structure

The "rad-hard" silicon photodiode structure is shown in Figure 2. This device was manufactured by Honeywell Spectronics in Richardson, Texas and is referred to as an "SPX-5000-047". This structure uses an n-type epitaxial layer as the optically active region. This active region is isolated from the substrate region by reverse biased p-n junctions. The thickness of this region is defined by the thickness of the epitaxial layer and can be selected to trade-off optical responsivity at a desired wavelength for ionizing-radiation insensitivity. The design of the device also reduces the regions of the device that are electrically active but optically inactive. This keeps the junction volume at a minimum for the application. These devices have not been coated with an anti-reflection material to reduce the amount of light reflected from the top surface. A glass spherical lens approximately 600 microns in diameter is attached to the top of the silicon photodiode die to increase the effective light collection cross-sectional area. The die was attached with approximately a 25 micron thick layer of RTV silicone. During the course of the experiments reported here, we never observed a darkening of the glass lens sphere due to irradiation or a mechanical failure at the lens-semiconductor bond.

Radiation Tests

Photocurrent measurements were made during exposure to three different pulsed irradiation sources. The following facilities were used for these tests: 1) The White Sands Missile Range linear accelerator (LINAC) which provided a 100 ns, 18 MeV

electron beam with an average dose rate of 10^7 - 10^{10} Rad (Si)/sec. 2) The Hermes II machine at Sandia National Laboratories which provided flash x-ray exposures with energies in the 1-10 MeV range during 54 ns pulses at dose rates of 10^{10} to 5 x 10^{11} Rad (Si)/sec. 3) Sandia National Laboratories Pulse Reactor Facility III (SPRF-III) which provided a simultaneous exposure to gamma rays (10^9 Rad (Si)/sec) and neutrons (4 X 10^{14} n/cm^2, E> 10keV), during a 100 usec pulse.

Special Photocurrent Measurement Circuitry

Special photocurrent measurement circuitry, shown in Figure 3, and careful cable shielding were used during these tests to minimize electromagnetic pulse (EMP) coupling effects and external radiation induced contributions to the measured signals. All sources of noise generated less than 1 mV in a 20 MHz bandwidth at the linear accelerator, less than 20 mV in a 100 MHz bandwidth at Hermes-II, and less than 0.3 mV in a 5 MHz bandwidth at SPRF-III. During our studies we observed three main sources of radiation induced current: photocurrent generated in the semiconductor under test, conduction effects in the ionized air during the pulse exposure (plasma currents), and Compton replacement current associated with charging and discharging of transmission cables. Careful experimental procedure was required to separate the contributions of each effect. Care was also taken to insure that the device under test was not significantly debiased by the voltage drop associated with the photocurrent measurement apparatus. The data was recorded on a transient waveform digitizer. The neutron irradiation studies at SPRF-III were primarily performed to investigate long term damage effects in photodiodes. These neutron irradiations were made on devices under electrical bias at the recommended operating voltage and on devices not electrically connected.

Optical Measurements

Optical responsivity measurements as a function of wavelength were made with a 0.44 m focal length, ruled grating type, double-monochromator system (SPEX #1672). The double-monochromator was used to insure a spectrally pure probe beam with minimal scattered light. The output of a high intensity quartz-halogen lamp (FDT-12V, 100W) was focused onto the entrance slit of the monochromator through order sorting filters to reduce the effects of high order diffraction contamination. A 50 micron aperture was postioned in front of the exit slit to reduce the illumination area of the photodiode so that the entire optical probe beam was incident only on the optically active region of the photodiode under test. The illuminated exit aperture was imaged on the photodiode under test with reflective optics to eliminate chromatic aberrations. A calibrated silicon photodiode (EG&G

550) and a pyroelectric radiometer (Laser Precision RK-5100) were used to measure the optical power incident on the test photodiode. No corrections were made for surface reflectivity in any of the reported measurements.

Results

Two sets of data will be examined here. The first collection of data shows the transient photocurrents induced during electron beam and x-ray irradiations. For many photodiode applications, it is important to minimize these currents to eliminate the transient upset caused by a nearby nuclear burst. The second set of data examined here illustrates the permanent effects of neutron exposures on photodiodes. These permanent effects generally result in a loss of optical sensitivity and an increase in the detector internal electrical noise level.

Before describing the results of these radiation studies, some discussion of the special "rad-hard" photodiode structure is appropriate. The AlGaAs/GaAs double heterojunction photodiode structure is shown in Figure 1. The use of direct bandgap semiconductor materials for device fabrication results in large optical absorption coefficients. This enables the fabrication of a thin device that efficiently collects a large percentage of the incident above bandgap optical photons. The total active volume thickness is less than one micron for these devices. Most of the optical energy of interest is absorbed within the top 0.5 microns of the GaAs active layer. The heterojunction structure creates internal electric fields which aid in the collection of the optical photon generated minority carriers and reject many of the ionizing-radiation generated minority carriers. In essence, this double heterostructure device has three important features to reduce the effects of ionizing-radiation: 1, The material is a direct bandgap semiconductor requiring small volumes for good optical collection. 2, The heterojunction structure creates internal electric fields which aid in the collection of optically generated minority carriers and tend to reduce the collection of ionizing-radiation generated minority carriers. 3, The relatively small distance between the edge of the depletion region and the average position of optical photon absorption reduces the dependency of the device on irradiation induced minority carrier diffusion length degradation.

The data compiled in Figure 4 shows the instanteous photocurent induced in several photodiodes by the White Sands linear accelerator electron beam. (Results from Hermes-II tests show results similar to the data from the linear accelerator.) The photodiodes were examined at several fluence levels as indicated on the horizontal axis. The induced photocurrent was found to vary approximately linearly with dose rate as expected but the photocurrent was found to vary somewhat non-linearly with device cross-sectional area. These

non-linear variations with device cross-sectional area are thought to be the result of the influence of plasma currents in the test fixtures and device package. Small area AlGaAs/GaAs devices are found to generate slightly more photocurrent than anticipated on the basis of test results from larger area devices. It is believed that the conduction paths in the air created by the pulsed ionizing-radiation add an extraneous conduction current component (plasma current) to the test results for the biased AlGaAs/GaAs photodiodes. In the larger area devices, the actual semiconductor photocurrent is much larger than the plasma current and the extra plasma component becomes insignificant. The silicon devices have a layer of RTV silicone that diminishes the plasma current effects.

This instantaneous photocurrent generated in photodiodes during exposure to a pulse of ionizing-radiation is a result of a combination of Compton scattering effects and the photoelectric effect, depending on the energy of the ionizing-radiation photon. Both mechanisms create excited electrons which generate many electron-hole pairs as the excited electrons move through the crystal lattice. These electron-hole pairs can contribute to the device current if they are created within approximately one diffusion length of the semiconductor depletion region edge. This ionizing-radiation induced photocurrent can be significantly larger than the intended signal current component, depending on the amplitude of the ionizing-radiation field and the amplitude of the signal intensity. By minimizing the active device volume, the magnitude of the radiation induced signal current can be reduced. Relatively short minority carrier diffusion lengths also decrease the number of ionizing-radiation induced minority carriers that contribute to the device current. Care must be taken not to make the active region thickness too narrow or the minority carrier diffusion length too small or the desired optically generated minority carriers will not contribute to the device current and the optical responsivity will be suboptimal.

In order to compare the radiation insensitivity of photodiodes fabricated from different materials with different dimensions and different optical sensitivities, a radiation response ratio figure of merit A_{rr} has been defined. The figure of merit A_{rr} is defined to be the ratio of the signal current density per unit of incident optical flux to the ionizing-radiation induced current density per unit dose rate. Note that for design considerations A_{rr}^2 is approximately proportional to the signal to noise power ratio in those systems where the ionizing-radiation induced photocurrent is the dominant noise factor. For the devices tested during this study and summarized in Figure 4, the A_{rr} value for the AlGaAs/GaAs double heterojunction photodiodes range from approximately 50 to 150 x 10^{-12} rad/optical photon. The silicon photodiode has an A_{rr} range of approximately 4. to 7.5 x 10-12 rad/optical photon for incident optical energy at 820

nm. The use of antireflection coatings on both devices could increase the values of A_{rr} by approximately 35%.

From an end user's perspective, the A_{rr} figure of merit can be translated into a system optical power requirement. In order to maintain the same signal to noise ratio during exposure to a pulse of ionizing-radiation, an optoelectronic data link using the silicon SPX-5000-047 photodiode would need approximately 10 - 25 times more optical power incident on the detector than an equivalent system with a double heterojunction AlGaAs/GaAs photodiode.

Neutron Studies

The data in Figure 5 and 6 shows the permanent degradation in optical responsivity after exposure to the SPRF III reactor at the indicated fluence. Our studies have shown that at normal operating bias voltages, the AlGaAs/GaAs photodiode suffered no degradation in optical responsivity after exposure to 3.6 x 10^{15} n/cm^2 and 900 krad as indicated in Figure 5. The Honeywell SPX-5000-047 silicon photodiode showed a 40% decrease in optical responsivity after 1.0 x 10^{15} n/cm^2 and 247 krad as shown in Figure 6. The 0 volt bias curves in Figures 5 and 6 indicate the approximate degradation in device optical responsivity for applications where the photodiodes were used in the photovoltaic mode. Both devices showed a slightly greater degradation at 0 volts bias, indicating the bias field (drift) collection of optically generated minority carriers was an important mechanism. Prior to the neutron irradiations optical responsivities were the same at bias (the photoconductive mode) and without bias (the photovoltaic mode). This effect is a result of neutron induced minority carrier diffusion length degradation.

The other prominent permanent effect resulting from neutron irradiation is an increase in photodiode dark current. Figure 7 illustrates the increase in photodiode dark (leakage) current after exposure to 1 x 10^{15} neutrons/cm^2 for the silicon device and 3.6 x 10^{15} cm^2 for the AlGaAs/GaAs device. The square root of the dark current level is proportional to one component of photodiode noise power. The internally generated noise of a photodiode is one of the main factors affecting the minimum optical power an optical detector can sense. This limitation determines the lower limit on the incident optical power before signal to noise ratios are unacceptable and error rates become too large. The data in Figure 7 shows that at the minimum operating bias (-20 volts) for the silicon device to maintain optical responsivity and response speed, the device dark current increases by a factor of approximately 7000 while the leakage current in the AlGaAs device (exposed to a greater neutron flux) increased by approximately a factor of 8 at a minimum operating bias of -2 volts. This difference in background noise level has significant impact on minimum allowable power levels in optoelectronic data links.

Neutron irradiation is believed to cause large clusters of disorder in the crystal lattice due to the relatively large energy transfer associated with neutron scattering. These disorder clusters in the crystal lattice create generation sites in the depletion region of the semiconductor junction. This causes an increase in the depletion layer generation-recombination current. This results in an increase in the photodiode dark (leakage) current and therefore a larger background noise level. The other important permanent damage effect from neutron irradiation is a reduction in optical sensitivity. The radiation induced defects created throughout the optically active volume tend to decrease the overall collection of optically generated minority carriers by reducing the minority carrier diffusion length. The crystal damage clusters serve as recombination sites causing optically generated hole-electron pairs to recombine before they can contribute to junction current.

LPE and MBE Device Characteristics

Finally we report here process improvements since our previously published work[1,2,3]. Electrical reverse bias characteristics of two AlGaAs/GaAs double heterojunction photodiodes are shown in Figure 8. Device # B392-2 was grown with liquid phase epitaxy (LPE) in a structure similar to Figure 1. The device active area was defined by a dicing saw process to approximately 2.0×10^{-3} cm^2; no mesa structure was used with this device. Device # M554-3-I was grown by molecular beam epitaxy (MBE); the structure for this device is shown in Figure 1. The M554 device has a photolithographically defined mesa active region with an area of approximately 2.0×10^{-3} cm^2. At a typical reverse bias operating condition of -3 volts, the MBE device has a dark current density of 5×10^{-8} A/cm^2; the LPE device at the same reverse bias has a dark current density of 5×10^{-4} A/cm^2. The improved characteristics are thought to be due to both the better quality material associated with the MBE growth process and the chemical mesa etch process. The chemical mesa formation is thought to create smoother surfaces at the edge of the junction region where the internal fields are the largest and irregular surfaces cause significant degradation in device breakdown voltage. The reverse bias breakdown voltage for the MBE mesa device is shown in Figure 8 to be in excess of 22 volts while the LPE sawed edge device has a 4.5 volt breakdown voltage. These results are significant for many applications in which noise currents (approximately proportional to the square root of leakage currents) determine the minimum detection levels. The expanded reverse bias range can be used to increase the photodiode speed of response.

Summary

We report here new results including the effects of neutron irradiation of AlGaAs/GaAs double heterojunction photodiodes and special, small active volume, PIN silicon photodiodes. Results from high energy electron irradiations are also presented. Finally we report on improvements in processing and growth of these radiation hardened, AlGaAs/GaAs, double heterojunction, photodiodes. Neutron irradiation studies have shown that the double heterojunction, AlGaAs/GaAs photodiodes degrade only slightly after exposure to 3.6×10^{15} neutrons/cm^2. The special "rad-hard" silicon PIN photodiodes showed consideralbly greater degradation in both optical responsivity and leakage current characteristics after exposure to neutron fluences of 1.0×10^{15} n/cm^2. Measurements of ionizing-radiation induced photocurrent during exposures to pulsed electron beams and pulsed x-rays show that the AlGaAs/GaAs structures generate only a fraction (.03 to .1) of the current generated by the small active volume, rad-hard, silicon photodiodes. Optimization of the device growth and fabrication processes have resulted in significantly better electrical characteristics while maintaining good optical properties.

The irradiation test results reported here expand our knowledge of the radiation hardness of these devices to include other types of irradiation threats beyond previously published work.

1. J.J. Wiczer, C.E. Barnes, & L.R. Dawson, "Transient Effects of Ionizing Radiation in Photodiodes", IEEE Trans. on Nucl. Sci., Vol. NS-28, #6, 1981, pp 4397-4402.

2. G.C. Osbourn, L.R. Dawson, & J.J. Wiczer, "Computer Modeling and Radiation Testing of AlGaAs Photodiode Structures", IEEE Trans. on Nucl. Sci., Vol. NS-28, #6, 1981, pp 4342-4345.

3. J.J. Wiczer, L.R. Dawson, G.C. Osbourn, & C.E. Barnes, "Permanent Damage Effects in Si and AlGaAs/GaAs Photodiodes", IEEE Trans on Nucl Sci, Vol. NS-29, #6, 1982, pp. 1539-1544.

Figure Captions:

Figure 1. This diagram illustrates the device structure of the double heterojunction, AlGaAs/GaAs radiation hardened photodiode.

Figure 2. This diagram illustrates the device structure of the small active volume, PIN silicon radiation hardened photodiode.

Figure 3. Schematic diagram of the electrical circuit used to measure photocurrent in photodiodes during exposure to pulsed ionizing-radiation.

Figure 4. Measured radiation induced current for several AlGaAs/GaAs and silicon photodiodes exposed to 18 MeV electrons from a linear accelerator.

Figure 5. Measured optical response degradation in AlGaAs/GaAs photodiode after exposure to neutron irradiation. Post-radiation measurements shown at 0 volts and -2 volts bias. Pre-radiation measurements were the same at 0 volts and -2 volts bias.

Figure 6. Measured optical response degradation in small active volume, silicon PIN radiation hardened photodiode structure after neutron irradiation. Pre-radiation measurements at 0 and -20 volts bias were the same.

Figure 7. Measured photodiode leakage current density before and after neutron irradiation. Note different neutron fluence levels used with silicon and AlGaAs/GaAs devices.

Figure 8. Leakage current and breakdown voltage characteristics for two AlGaAs/GaAs photodiodes with identical vertical structures but different process and growth technologies. Device #B-392 was grown with a liquid phase epitaxy process and used a crude saw cut to isolate devices on wafer. Device # M- 554 was grown with molecular beam epitaxy and used a chemical mesa etch process to isolate individual devices on the wafer.

Figure 1

RADIATION – HARDENED PHOTODIODE

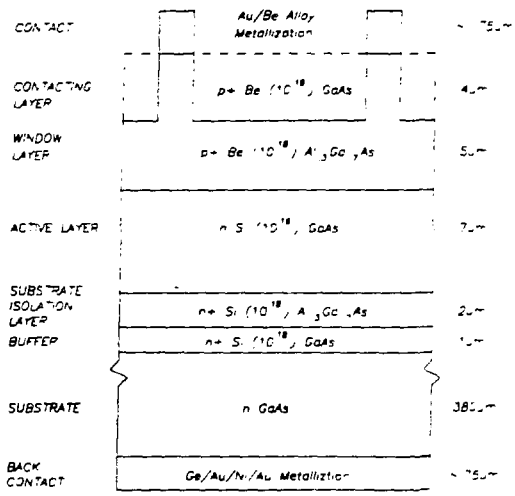

Figure 2

SILICON RAD HARD PHOTODIODE

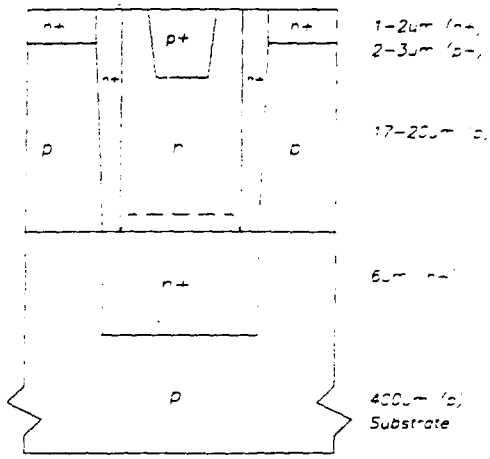

Figure 3

PHOTOCURRENT MEASUREMENT APPARATUS INCORPORATING CURRENT VIEWING RESISTOR

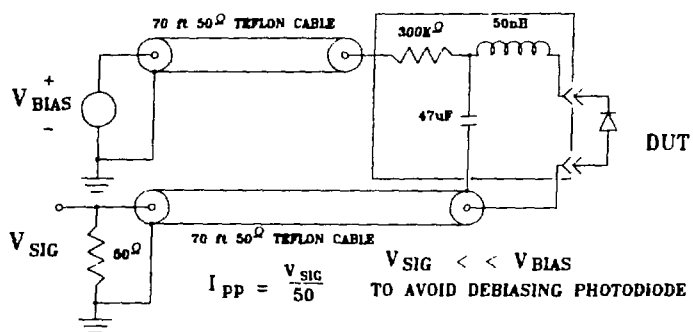

Figure 4

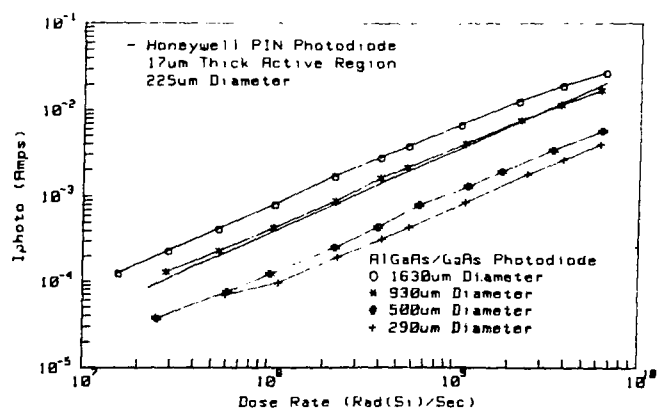

Figure 5

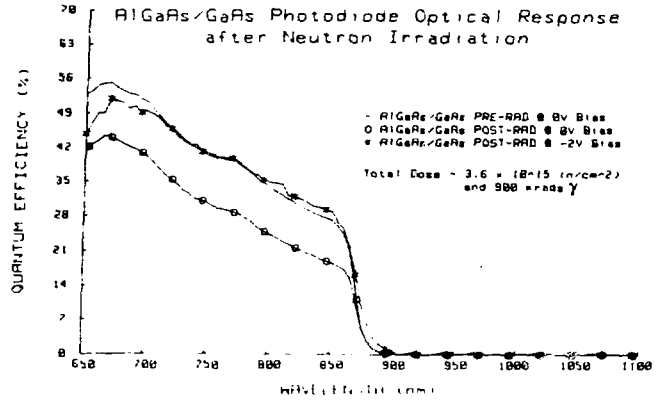

Figure 6

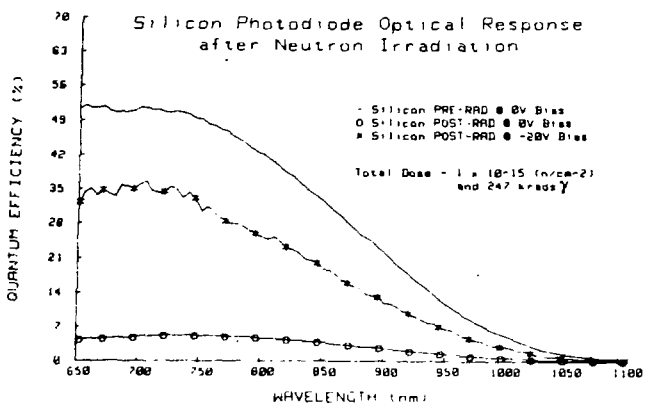

Figure 7

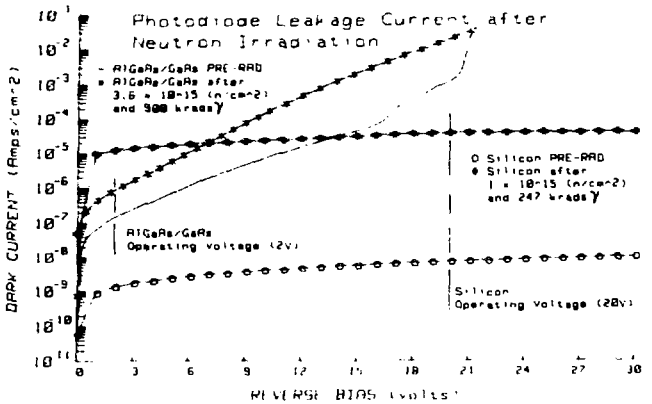

Figure 8